JOURNAL OF THE ROYAL SOCIETY Interface

J. R. Soc. Interface (2007) **4**, 1077–1092
doi:10.1098/rsif.2007.0227
Published online 20 March 2007

An integrated systems biology approach to understanding the rules of keratinocyte colony formation

Tao Sun[1], Phil McMinn[2], Simon Coakley[2], Mike Holcombe[2], Rod Smallwood[2] and Sheila MacNeil[1,*]

[1]*Department of Engineering Materials, and* [2]*Department of Computer Science, University of Sheffield, Kroto Research Institute, Broad Lane, Sheffield S3 7HQ, UK*

Closely coupled *in vitro* and *in virtuo* models have been used to explore the self-organization of normal human keratinocytes (NHK). Although it can be observed experimentally, we lack the tools to explore many biological rules that govern NHK self-organization. An agent-based computational model was developed, based on rules derived from literature, which predicts the dynamic multicellular morphogenesis of NHK and of a keratinocyte cell line (HaCat cells) under varying extracellular Ca^{++} concentrations. The model enables *in virtuo* exploration of the relative importance of biological rules and was used to test hypotheses *in virtuo* which were subsequently examined *in vitro*. Results indicated that cell–cell and cell–substrate adhesions were critically important to NHK self-organization. In contrast, cell cycle length and the number of divisions that transit-amplifying cells could undergo proved non-critical to the final organization. Two further hypotheses, to explain the growth behaviour of HaCat cells, were explored *in virtuo*—an inability to differentiate and a differing sensitivity to extracellular calcium. *In vitro* experimentation provided some support for both hypotheses. For NHKs, the prediction was made that the position of stem cells would influence the pattern of cell migration post-wounding. This was then confirmed experimentally using a scratch wound model.

Keywords: computational modelling; keratinocyte; HaCat cell; calcium; wound healing; individual-based model

1. INTRODUCTION

In recent years, it has been proposed that the development of a complex tissue is crucially dependent on the coordination of relatively few mechanisms (Nishimura *et al.* 1999; Eglen & Willshaw 2002; Galle *et al.* 2005; Vespa *et al.* 2005). The explanation for this is that many biological processes on the sub-cellular scale appear to interact at the cellular or the multi-cellular level (Aplin *et al.* 1999; Ingber 2003*a*,*b*).

Previously, we developed a cell-based computational model of the growth characteristics of urothelial cells in monolayer culture in low or physiological levels of calcium, which gives a qualitative fit to *in vitro* cell behaviour (Walker *et al.* 2004*a*,*b*). Extension to normal human keratinocytes (NHK) and a keratinocyte cell line (HaCat) indicated that although this model can describe the effect of extracellular calcium on NHK proliferation and differentiation, it is not sufficient to simulate the colony formation of keratinocytes and it also failed to model the behaviour of HaCat cells in response to changing extracellular calcium (Walker *et al.* 2006). The aim of this study was to further develop the model to explore how NHK self-organize into an epithelium—particularly how they form colonies. The motivation is that, while there is growing knowledge of how individual cells respond from the genome through to the proteome and metabolome, it is difficult for biologists to integrate all the information and regenerate a holistic view of the organism (Rashbass 1996; Galle *et al.* 2005). Computational modelling provides a powerful tool to handle this complexity and can improve our understanding of tissue morphogenesis and pathogenesis (Rashbass 1996; Morel *et al.* 2001; Galle *et al.* 2005; Ponciano *et al.* 2005).

A modelling approach which is gathering popularity with biologists is the use of agent-based models. Each individual cell is represented by a software agent. In this particular model, the software agents are a form of communicating X-machine (Balanescu *et al.* 1999; Kefalas *et al.* 2003). Each agent has a rule set, based on experimental cell biology, which determines the behaviour of the agent and its interaction with its neighbours. The interaction of a set of agents (which are equivalent to a cell population) can be used to model the organization of multicellular aggregates (Walker *et al.* 2004*a*; Grabe & Neuber 2005). The model is implemented using the FLexible Agent-based Modelling Environment (FLAME) which is available at http://www.flame.ac.uk. The attraction of this approach is that it is capable of connecting

*Author for correspondence (s.macneil@sheffield.ac.uk).

Received 31 January 2007
Accepted 22 February 2007

experimental results to fundamental principles of biological behaviour and can explore the influence of a single parameter on the behaviour of a biological system, a scenario often unattainable in *in vitro* or *in vivo* experimentation. It is particularly useful for identifying key parameters that play a central role in defining the overall behaviour of a biological system, and in this respect can lead to new and more informative experiments (Olsson 2003; MacArthur *et al.* 2004; Drasdo & Hohme 2005; Zaman *et al.* 2005). It can open new perspectives to process the huge amount of data provided by experiments and to separate generic principles of organization from cell-specific characteristics (Rashbass 1996).

With respect to the human epidermis, the knowledge base is relatively mature. Normal human keratinocytes constitute over 80% of the cells in interfollicular epidermis which is a rapidly renewing tissue (Holbrook 1994). It is known that cells are shed at the skin surface and are replaced by the division in the basal layers of the epidermis, known as the germinative compartment (Webb *et al.* 2004). Evidence suggests that cells in the basal layer are heterogeneous in type and have a hierarchical population structure (Laporte & Heenen 1994; Jensen *et al.* 1999; Webb *et al.* 2004). Over the last 15 years, a considerable volume of data about the regulation of epidermal stem cells and cell proliferation have been collected. The approach for this study was to use areas of strong consensus in epithelial biology literature as the basis for the initial rule set for governing cellular behaviour. Thus, the behaviour of the software agents was based on generic rules for cell division, migration, differentiation and signalling. The interaction of the software agents (*in virtuo* cells)—their emergent behaviour—describes the macroscopic morphogenesis of NHK *in vitro*. The generic properties were then investigated by varying parameters and by selective *in virtuo* knockout of the mechanisms to describe the growth behaviour of a transformed keratinocyte cell line (HaCat cells). After validation of the *in virtuo* model by comparison with *in vitro* behaviour, the model was then used in a predictive sense. For NHK, we hypothesized that the spatial distribution of cells in mature colonies would influence the pattern of wound healing if deliberate wounds (scratch wounds) were made in NHK cell cultures. For HaCat cells, we explored two hypotheses that cells basically lacked the ability to self-regulate colonies and differentiate or that an insensitivity to extracellular calcium might explain most (if not all) of the abnormal differentiation pattern of these cells. *In vitro* experiments proposed from these predictions were then carried out to confirm or refute these predictions.

In §§§§2–5, we summarize the development of the model, firstly describing the materials and methods of *in vitro* experiment, introducing the concept of agent-based modelling, secondly the literature research evidence on which the rule mechanisms for NHK behaviour were based and thirdly how these were applied to the model. Results from this model both *in virtuo* and *in vitro* are then presented followed by a discussion of these.

2. MATERIALS AND METHODS

2.1. Cell culture

The methodology of NHK isolation and culture and assessment of involucrin by immunofluorescence microscopy were as described previously (Sun *et al.* 2005).

2.2. In vitro *scratch wound assessment*

Confluent NHK cells were cultured in low (0.09 mM) or physiological (2 mM) Ca^{++} media for varying periods of time in six-well tissue culture plates. Scratch wounds were then made across the centre of each well using a 600–800 μm wide sterile pipette tip. After removing debris by re-feeding the cells with fresh media, migration of cells into the denuded areas was analysed by photographing and measuring the distance between the two wound edges at different time points using a phase contrast microscope (Leica, Germany) and image analysis software (Openlab v. 4.0.2 and Volocity v. 3.0.2, Improvision, UK). In order to photograph the same field at each time point, the underside of culture dishes were labelled with letters on the bottom of each well to act as a reference point for scratch wound assessments.

2.3. Bromodeoxyuridine immunofluorescence microscopy

Incorporation of bromodeoxyuridine (BrdU) into DNA during the S phase of the cell cycle was used to show cell proliferation. Briefly, after incubation in BrdU labelling medium (Roche) for 6 h at 37°C, the cells were fixed in ethanol and 50 mM glycine fixative (in 7 : 3 ratio) at −20°C for 20–30 min. After removal of the fixative and thoroughly washed thrice with PBS, cells were incubated with anti-BrdU monoclonal antibodies (Roche, 1 : 300 dilution) for 30 min at 37°C, fluorescein-conjugated anti-mouse secondary antibodies (1 : 500 dilution) for 30 min at 37°C, DAPI (to stain nuclei; 1 : 1000 dilution) for 15 min and washed thoroughly with PBS thrice after each incubation.

Epifluorescence images of immunostained cells were taken with an ImageXpress (AXON, USA) at $\lambda_{ex} = 495$ nm, $\lambda_{em} = 515$ nm (for FITC/BrdU, involucrin visualization) and $\lambda_{ex} = 358$ nm, $\lambda_{em} = 461$ nm (for DAPI/nuclei visualization).

3. DEVELOPMENT OF THE AGENT-BASED MODEL

3.1. Introduction to agent-based modelling

Agent-based modelling is based on the behaviour of individual entities, their environment and the rules that govern their behaviour, rather than from a mathematical description of the average behaviour of a collection of entities. From the interaction of these basic entities, group behaviours emerge. It allows for a population of heterogeneous agents (in this case a population of *cells* modelled using a form of communicating X-machines; Balanescu *et al.* 1999) with varying position and internal state (Walker *et al.* 2004*a*; Grabe & Neuber 2005).

An agent-based model is composed of two parts: the *agents*, in this case representing *cells*; and the *environment*, here being the culture dish in which the cells reside, along with global factors such as extracellular calcium. Each cell was modelled as a non-deformable sphere of 20 μm in diameter, which was capable of migration, proliferation and differentiation. The culture dish was modelled as a user-defined flat, square surface with 'walls'. For the purposes of these experiments, the dish was 500 μm in dimension with a wall height of 100 μm. The exogenous calcium level was set as variable in the range of 0.09–10.0 mM.

The model framework used was that of Coakley *et al.* (2006). Each cell is represented by an individual agent. Agents communicate (cell signalling) by reading and writing to message lists. The process can be represented by the following pseudocode:

```
For each time-step
  For each agent
    Read state and position of neighbouring agents
    from message list
    Update state and position as determined by
    internal rules and external signals
    Write new state and position to message list
  End
End
```

The framework used, (FLAME, http://www.flame.ac.uk), provides automated tools for generating software in the language C which is highly efficient and capable of being run on supercomputers if required.

Each iteration in this model represents a time-step of 30 min. The rule sequence is as shown in figure 1*a*. Initially, agents (cells) output their location and type (1=stem cell; 2=transit amplifying (TA) cell; 3=committed cell; 4=corneocyte) to the message lists for other cells to read. Each cell then performs rules specific to its own position in the cell cycle. Following this, cells decide whether to change to another cell type based on the differentiation rules in the model. Cells then execute their migration and physical rules. All rules are executed in the context of the agent's own internal state and its immediate environment as discovered through interrogation of the message lists.

Sections 3.2–3.7 describe the rules of the model in greater detail.

3.2. Stem cells to corneocytes

Current literature supports the view that epithelial cells in skin exist in one of the four states (stem cells, TA cells, committed cells and corneocytes). Stem cells are said to comprise approximately 5% of the human adult epidermis with an indefinite lifespan and they are capable of giving birth to stem or TA cells (Savill & Sherratt 2003; Okuyama *et al.* 2004; Webb *et al.* 2004). TA cells are estimated to be capable of dividing no more than 3–5 times. Once they stop dividing, they are categorized as post-mitotic or committed cells (Dover & Wright 1991; Jensen *et al.* 1999; Lowell *et al.* 2000; Okuyama *et al.* 2004; Kolly *et al.* 2005). Normally committed cells are referred to as undifferentiated

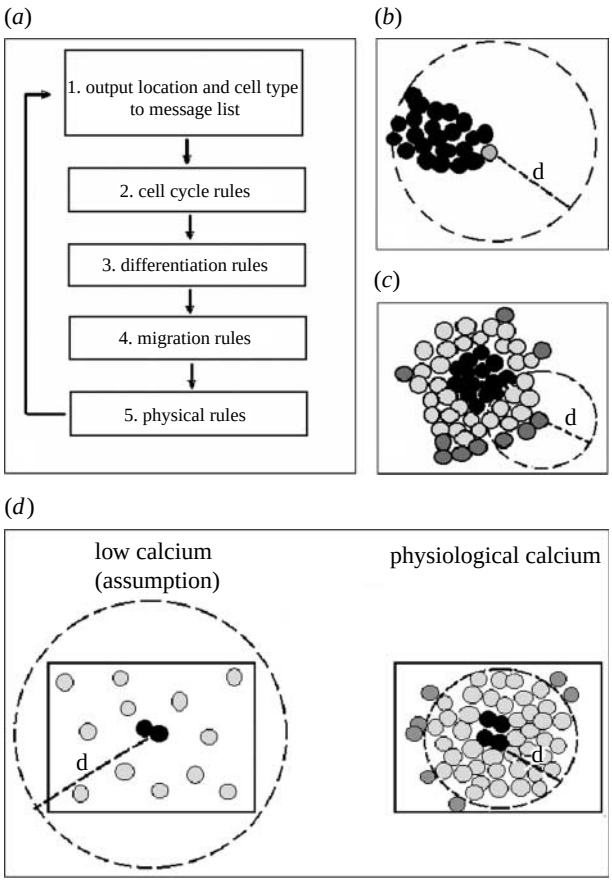

Figure 1. (*a*) Rules performed by each cell in each iteration. (*b*) Differentiation rules from stem cell (black) to TA cell (light grey). If the stem cell number goes above a threshold and the number of stem cell contacts is relatively low (indicating it is on the edge of the niche), the stem cell differentiates into a TA cell. (*c*) Differentiation rules from TA cell (light grey) to committed cell (dark grey). If a TA cell cannot find a stem cell (black) within a certain radius in three dimensions (out of the stem cell protection region), it commits. (*d*) The different radii used by stem cells (black) and TA cells (light grey) depend on the global factors including exogenous calcium concentration. Distance constants used in differentiation rules are set according to the calcium levels: in low Ca^{++} environments, the distance was assumed to be larger than the size of normal cell culture vessels; in physiological Ca^{++} environments, the distance based on the *in vivo* or *in vitro* data.

cells which have initiated, but not completed their differentiation programme. These cells are found in the basal layer and superbasal layer. Keratinocytes in the spinous and granular layers of epidermis are progressively more differentiated (Grabe & Neuber 2005). In this research, the term 'committed cell' is used as an umbrella term to cover not just the post-mitotic cells in the basal layers but all the cells between TA cells and corneocytes at different differentiation stages. Therefore, the committed cells in the model represent all the cells that are destined to move upwards from the basal layer by a process that involves down-regulation of integrin expression and function, withdrawing from the cell cycle, undergoing terminal differentiation and finally desquamating at the skin surface as corneocytes (Latkowski *et al.* 1995; Jensen *et al.* 1999; Zhu *et al.* 1999; Savill & Sherratt 2003).

3.3. Application of skin cell division rules to the model

Stem cells have an unlimited self-renewal capacity (Jensen *et al.* 1999; Potten & Booth 2002) and TA cells are capable of division before being committed to differentiation (Savill & Sherratt 2003). Accordingly, for modelling purposes, both cells were assumed to proliferate and re-enter the cell cycle after every preceding birth was fully completed until they were contact inhibited or received differentiation signals (as discussed in §§ 3.4 and 3.5). A cell will enter the resting phase (G0) if it becomes contact inhibited. The agent interrogates the message lists to find the number of neighbours in its immediate vicinity. If the number of cells is more than x, then the cell enters G0. When the number of neighbouring cells falls below x again, the cell leaves G0 and restarts countdown to division until the cell stays in G0 longer than a certain period of time. The number of neighbouring cells needed to trigger contact inhibition and initiate differentiation depends on the cell type and exogenous Ca^{++} level as discussed in §§ 3.4 and 3.5 on differentiation rules.

There are no conclusive, independent cell cycle measurements of stem and TA cells in human epidermis. Measured cell cycle times vary between 30 and 300 h, with the average being 60 h (Dover & Potten 1983; Savill 2003). Although TA cells were reported to divide at a faster rate than stem cells *in vivo*, both cells were reported to divide at the same rate *in vitro* (Savill & Sherratt 2003). In this model, the intrinsic cell cycle times designated to TA and stem cells were 30 h (60 iterations) and 60 h (120 iterations), respectively, which can be prolonged due to possible growth arrests.

3.4. Physical distribution and differentiation of skin cells

Evidence suggests that stem cells aggregate to form patches or clusters, which have a specific location with respect to the epidermal–dermal junction (Jensen *et al.* 1999; Lowell *et al.* 2000; Savill & Sherratt 2003). The cell number of each stem cell niche has been estimated to be at least 20, probably up to 40 (Asplund *et al.* 2001; Savill & Sherratt 2003). This regular distribution of stem and TA cells is thought to be subject to autoregulation and can be recreated in cell culture (Jensen *et al.* 1999; Savill & Sherratt 2003).

Two cell adhesion molecules (CAM), β1 integrin and Delta 1, evolved in the autoregulation of the stem cell colony, are currently used to locate stem cell niches. Stem cells express approximately twofold higher levels of β1 integrin and Delta 1 than TA cells (Jensen *et al.* 1999; Zhu *et al.* 1999; Lowell *et al.* 2000; Savill & Sherratt 2003). The high β1 integrin level and consequently strong adhesive characteristics of stem cells are thought to be required to prevent entry into the TA cell compartment (Jensen *et al.* 1999; Zhu *et al.* 1999; Lowell *et al.* 2000). High Delta 1 expression has been reported to protect stem cells by blocking Notch signalling, enhancing cell–cell cohesiveness and inducing the cells on the colony edge to differentiate (Lowell *et al.* 2000; Savill & Sherratt 2003). Although epidermal stem cell number is thought to be subject to autoregulation, there is also evidence that environmental factors, specifically the composition of the basement membrane (Aplin *et al.* 1999; Zhu *et al.* 1999) and the presence of neighbouring keratinocytes (Lowell *et al.* 2000; Okuyama *et al.* 2004) play important roles in establishing and maintaining the patterned distribution of stem cells within the epidermal basal layer. The effect of different factors on cell pattern formation are also found in other cell types (Bhadriraju & Hansen 2004; Nelson *et al.* 2005; Shraiman 2005).

Exit from the cell cycle and initiation of differentiation is thought to be under the control of many factors of which Notch 1 and c-Myc are key regulators (Zhu *et al.* 1999; Kolly *et al.* 2005). These are both triggered by cell confluence and are mutually exclusive (Kolly *et al.* 2005). At cell confluence, Notch 1 is activated and c-Myc is inhibited and their cell–cell signalling pathways are thought to trigger cell cycle exit followed by transcriptional upregulation of p21/p27 and the onset of terminal differentiation (Kolly *et al.* 2005). *In vitro* research also shows that there is a requirement for a certain level of extracellular (and by implication intracellular) calcium to reinforce the initiation of terminal differentiation and allow it to proceed to completion. Thus, the onset of terminal differentiation was observed to occur but failed to complete in low Ca^{++} environments (Okuyama *et al.* 2004; Kolly *et al.* 2005). Additionally, many other factors have been reported to trigger differentiation of human and mouse keratinocytes, e.g. TGF-β, forced expression of PKC and detachment of cells from the substrate (Sakaguchi *et al.* 2003). Therefore, calcium is treated as one of the several factors to trigger keratinocyte differentiation in this research, while in the earlier model of Grabe & Neuber (2005) calcium is considered the key factor responsible for keratinocyte differentiation.

3.5. Application of skin cell differentiation rules to the model

The following differentiation mechanisms were explicitly modelled: (i) contact inhibition (Galle *et al.* 2005), (ii) presence of differentiation/apoptosis signals, such as ceramide (Kolettas *et al.* 2006), Fas (FasL; Ashkenas *et al.* 1996; Wang *et al.* 2004) and elevated extracellular Ca^{++} concentration (Grabe & Neuber 2005), (iii) absence of protective signals (Ashkenas *et al.* 1996), (iv) simultaneous signals of growth and differentiation (King & Cidlowski 1995; Thompson 1995; Ashkenas *et al.* 1996), (v) loss of cell–matrix and or cell–cell contacts (Adams & Watt 1990; Ashkenas *et al.* 1996; Assoian 1997; Santini *et al.* 2000; Grossmann *et al.* 2001), and (vi) remaining in a quiescent state (G0) for longer than a certain period of time as used by other models (Drasdo & Hohme 2005).

CAM-mediated cell–cell contact not only inhibits (Croix *et al.* 1998; Orford *et al.* 1999; Gizelda *et al.* 2000) but also enhances cell proliferation (Bhatia *et al.* 1999; Nelson & Chen 2002). Epithelial cells with strong cell–cell contacts were found to survive longer even after losing substrate contact (Santini *et al.* 2000).

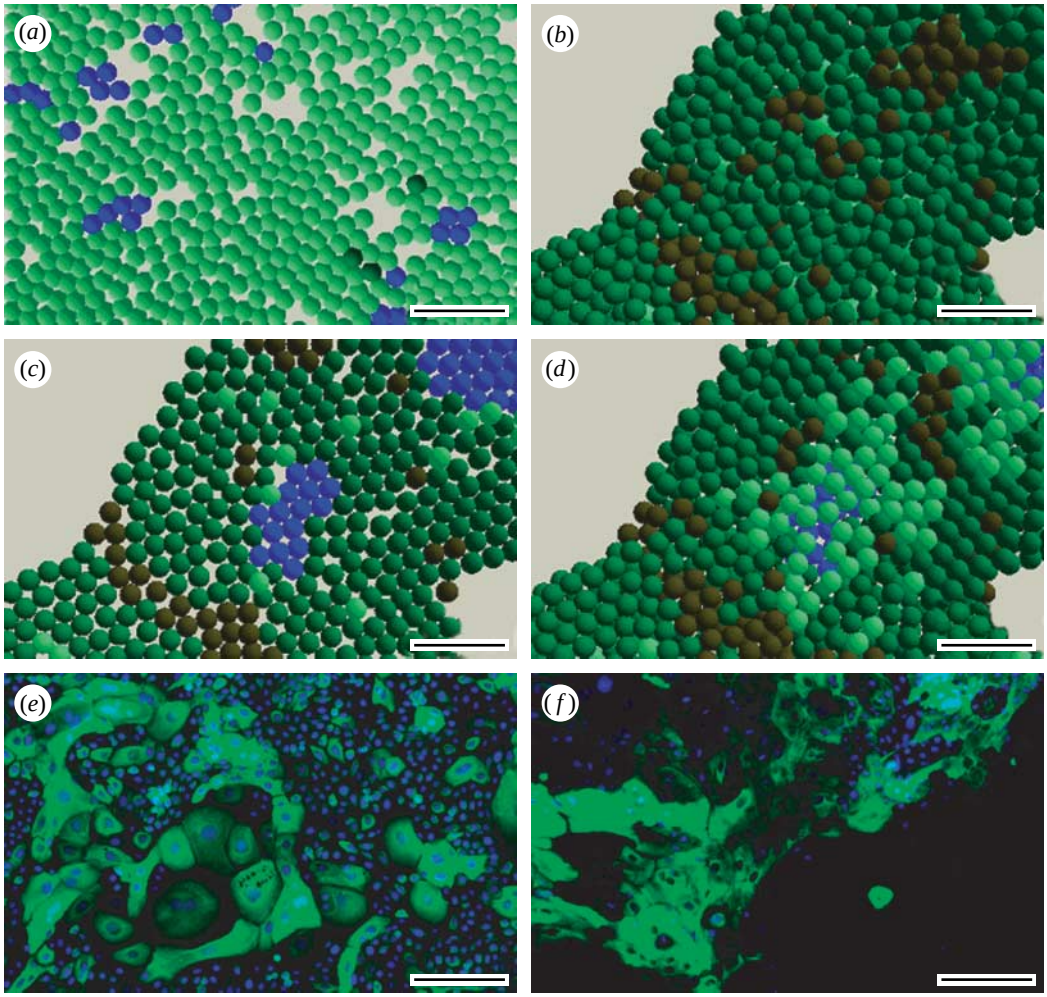

Figure 2. Micrographs of modelled keratinocytes in (*a*) low and (*b–d*) physiological Ca^{++} environments, (*b*) shows an overview of a colony, (*c*) the appearance of the basal layer and (*d*) the appearance of the middle layer of cell for the same colony. The modelled cells are stem cells (blue), TA cells (light green), committed cells (dark green) and corneocytes (brown). Fluorescent micrographs of NHK cultured in (*e*) low and (*f*) physiological Ca^{++} environments. The cells were stained with DAPI (blue) and pancytokeratin antibody (green). Scale bar, 100 μm.

Therefore, confluence-regulated cell contact inhibition or stimulation must be considered in a broader biological context (Scheffrahn *et al.* 2005; Walker *et al.* 2005). In a low Ca^{++} environment, individual cells are less stimulated as the result of weak cell–cell contact, therefore, fewer neighbouring cells were needed to trigger contact inhibition. In a physiological Ca^{++} environment, individual cells are stimulated by strong cell–cell interactions and are assumed to require more neighbouring cells to become contact inhibited.

Stem cells are thought to be able to generate local niches by expressing specific basement membrane components (Korang *et al.* 1995; Smola *et al.* 1998; Fleischmajer *et al.* 2000) and higher levels of growth factors and/or corresponding receptors (Morel *et al.* 2001), which can stimulate and maintain the proliferation of cells inside or close to the niches. This protection effect is inversely proportional to the distance between the affected cells and the niches in three dimensions. Consequently, TA model cells near the niches are constantly undergoing division. As they escape the protective region, they are less proliferative and start to differentiate, which is also reinforced by differentiation or apoptosis signals (Morel *et al.* 2001). The protection effect also depends on global factors, since large NHK colonies can be obtained in highly supplemented culture medium (Goulet *et al.* 1996). In this model, the protection effect was assumed to be inversely proportional to the elevated Ca^{++} level. In a low Ca^{++} media, the longest protection distance (assumed to be larger than the size of normal cell culture vessels) was applied as almost all the cells were observed to behave as TA cells (Dalrymple *et al.* 2005).

The differentiation rules in the model centre on the formation of colonies. Through cell division, stem cell colonies are formed from stem cells initially seeded by the user. Stem cell colony size is subject to autoregulation (Jensen *et al.* 1999; Zhu *et al.* 1999; Lowell *et al.* 2000; Savill & Sherratt 2003). Based on the literature and experiments, we assumed there was a bell-shape relationship between stem cell cluster size and exogenous Ca^{++} level (Asplund *et al.* 2001), with a maximum size at physiological Ca^{++} level (Sakaguchi *et al.* 2003). Consequently, when the cluster size is reached at a certain Ca^{++} concentration, cells on the edge of the stem cell colony differentiate into TA cells, which give birth to further TA cells. This is implemented as follows. A stem

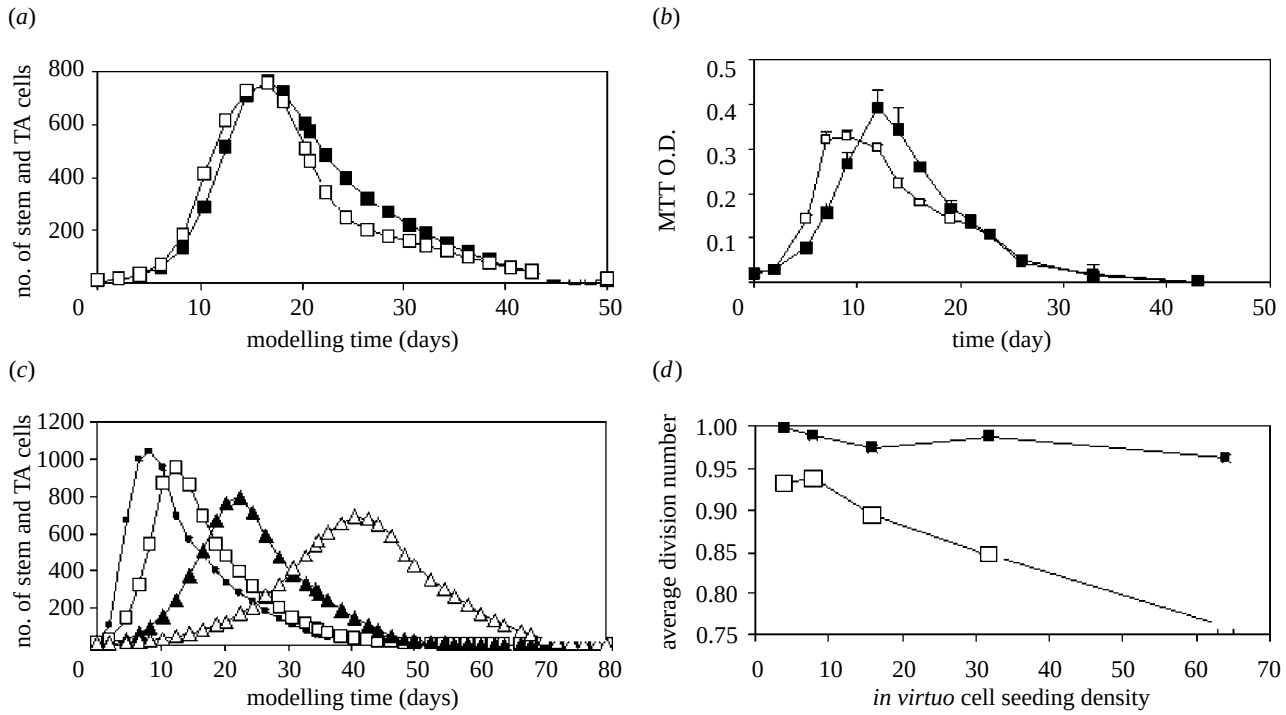

Figure 3. (*a*) Growth curves of modelled stem and TA cells of keratinocytes simulated in low (open square, 0.09 mM) and physiological (filled square, 2 mM) Ca^{++} environments. (*b*) Growth curves of *in vitro* NHK measured with MTT-ESTA assessment cultured in low (open square, 0.09 mM) and physiological (filled square 2 mM) Ca^{++} environments. (*c*) Effect of different cell cycle times (filled square, 30 h; open square, 60 h; filled triangle, 120 h; open triangle, 240 h) of TA and stem cells on the growth curve of the total number of stem and TA cells modelled in physiological Ca^{++} (2 mM) environments. (*d*) Effect of different cell seeding density on the average division number of TA cells simulated in low (open square, 0.09 mM) and physiological (filled square 2 mM) Ca^{++} environments.

cell simulates real-life signalling mechanisms by examining the message lists and checking the number of stem cells in its vicinity within a certain radius. If the figure goes above a threshold, and the number of stem cell contacts is relatively low (indicating it is on the edge of the niche), the cell differentiates into a TA cell (figure 1*b*).

TA cells in the model undertake a similar process as to whether they should differentiate into a committed cell by monitoring message lists for stem cells. If a TA cell cannot find a stem cell within a certain radius in three dimensions (out of the stem cell protection region), it commits (figure 1*c*). The different radii used by stem cells and TA cells depend on the global factors including exogenous calcium concentration as discussed above (figure 1*d*). The committed cells gradually lose their nuclei and further differentiate to corneocytes. Both committed cells and corneocytes also send out differentiation/apoptosis signals (e.g. ceramide and or Fas/FasL) to the neighbouring cells. Both TA and stem cells are committed to differentiate if certain number of neighbours are differentiated cells and/or corneocytes.

As keratinocytes are shed from the skin surface and any apoptosis seen was observed at a very low level in the human epidermis (Savill 2003), apoptosis was not explicitly modelled.

3.6. Experimental evidence used for migration rules

Cell motility is largely due to the cell–substrate and cell–cell interactions. There is a bell-shaped relationship between cell migration speed and integrin-mediated cell–substrate contact, with maximum migration rates at intermediate cell–substrate adhesiveness (DiMilla *et al.* 1991; Jensen *et al.* 1999; Cox *et al.* 2001). Cell motility can be opposed by cadherin-based cell–cell adhesion (Lowell *et al.* 2000). TA cells have a higher motility than other cell types (Jensen *et al.* 1999) and isolated TA cells were observed to perform a random walk-like movement in low Ca^{++} environments. A migration speed of approximately 1 $\mu m\ min^{-1}$ was selected for TA model cells in low Ca^{++} media based on time lapse experiments. Migration was assumed to be inversely proportional to the Ca^{++} level. It is thought that the essential mechanism responsible for epithelial cell flux is mitotic activity, which causes a pressure-driven passive movement (Jensen *et al.* 1999; Meineke *et al.* 2001).

3.7. Physical rules for cell interactions

The physical rules consist of attractive and repelling forces between agents in the model. A movement is then applied to each agent corresponding to the forces acting on it. As the actions of cell migration and division are modelled as discrete steps that are applied to each agent individually, it is possible for the simulated cells to overlap on their virtual culture plate. In this instance, a corrective repulsive force is applied in order to push the cells apart. This is proportional to the overlapping area (a higher force for a bigger overlap). Attractive forces simulate bonds between cells and the substrate, and are applied when the respective bodies (cell–cell or cell–substrate) are within 10 μm of one

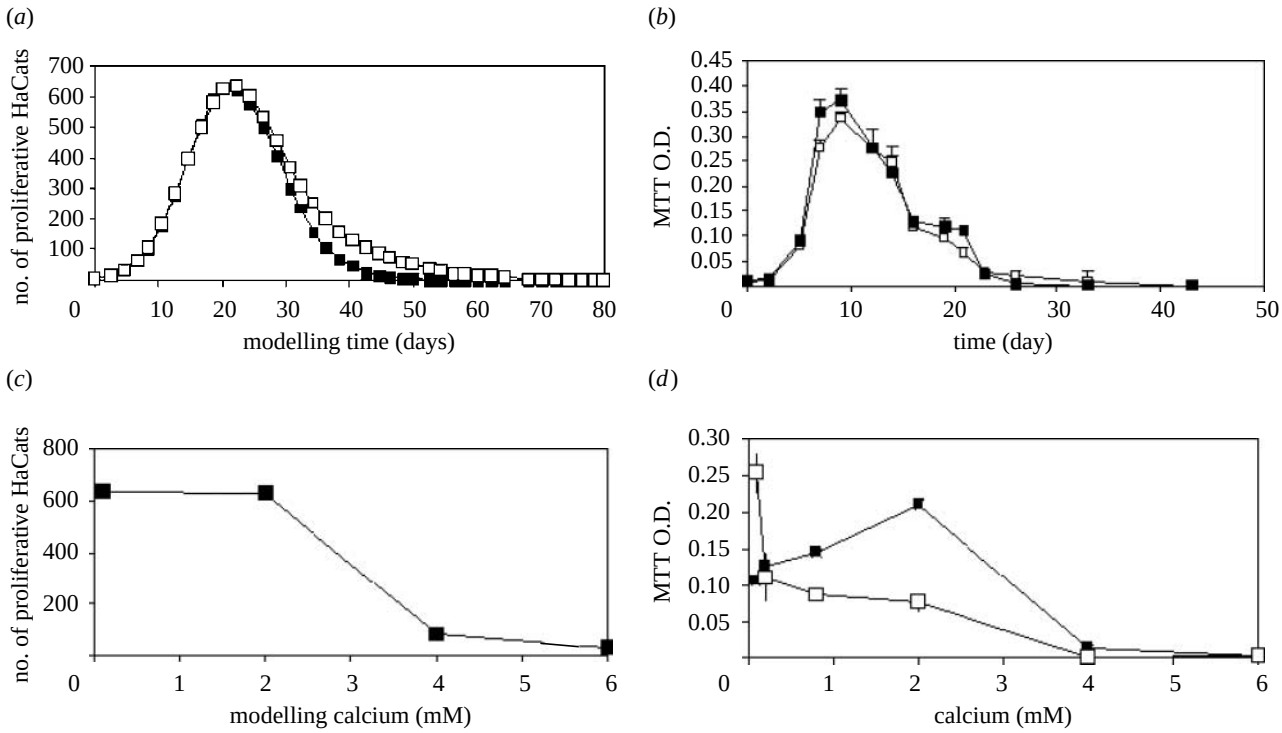

Figure 4. Growth curves of (*a*) modelled HaCat cells and (*b*) *in vitro* HaCat cells measured with MTT-ESTA assessment that simulated or cultured in low (open square 0.09 mM) and physiological (filled square 2 mM) Ca^{++} environments. (*c*) Total number of modelled HaCat cells simulated in different Ca^{++} environments. (*d*) MTT-ESTA assessed overall cell viability of HaCat cells (filled square) and NHKs (open square) cultured in different calcium environments.

another. Bond strengths depend on the individual type of cells involved and are related to the environmental calcium concentration (Lowell *et al.* 2000) via a sigmoid function (Baumgarter *et al.* 2000).

In low Ca^{++} media, cells (most of which are TA cells) have low cadherin-mediated cell–cell and integrin-based cell–substrate bonds. In a physiological Ca^{++} environment, stem cells exhibit strong cell–cell and cell–substrate bonds due to high levels of Delta 1 and integrins (Jensen *et al.* 1999; Lowell *et al.* 2000; Savill & Sherratt 2003). Committed cells and corneocytes in physiological Ca^{++} form strong cell–cell and cell–substrate bonds through desmosomes and hemidesmosomes (Okuyama *et al.* 2004; Kolly *et al.* 2005) and age-related upregulated E-cadherin expression (Morel *et al.* 2001). TA cells have the lowest cell–cell or cell–substrate bonds due to the low level of Delta 1, integrins and E-cadherin. Cells and neighbouring cell spheres (or substrates) form contacts sharing a common, flat contact area. In this model, the cell–cell or cell–substrate adhesion was deliberately set within the range of 0–1, with a higher number representing stronger bonds. This allowed for *in virtuo* exploration of the bond strengths on an empirical basis to simulate *in vitro* behaviour of cells.

The code for the model itself will be made available from: http://www.flame.ac.uk.

4. RESULTS

4.1. Simulation of NHK dynamic multicellular morphogenesis

As illustrated in figure 2*a*, in a low calcium environment, following the rules described in the methods, the stem cells divided symmetrically 2–3 times, then asymmetrically to produce TA cells. TA cells divided, migrated randomly and distributed evenly over the substrate. After the culture achieved confluence, the cells withdrew from the cell cycle due to confluence triggered contact inhibition and gradually lost viability. No stratification occurred as cells maintained high cell motility and only four neighbouring cells were needed to induce contact inhibition. In a physiological calcium environment (as shown in figure 2*b–d*), a heterogeneous cell composition and hierarchical population structure were reproduced by the model. Stem cells kept dividing symmetrically in compact clusters before the targeted colony size was obtained. After that, the stem cells on the colony edge started to give birth to a stem and a TA cell due to the cluster autoregulation mechanism proposed. TA cells near the stem cell niches were observed to proliferate, migrate and stratify actively. When TA cells escaped the influence of stem cells, they differentiated to committed cells and eventually changed to corneocytes. Due to the strong cell–cell and cell–substrate adhesiveness, differentiated NHK cells formed a tight shell around TA and stem cell compartments as shown in figure 2*b*. Figure 2*c* depicts the basal layer for the colonies seen in figure 2*b*, and figure 2*d* a middle layer of cells in the same colony (The model allows the colonies to stratify for up to four layers). The differentiation of TA and stem cells was also initiated by their neighbouring committed cells through synthesis of differentiation signals (e.g. ceramide and Fas/FasL) and/or establishment of local confluence. (Please see the website http://www.dcs.shef.ac.uk/~phil/epiresources for movie clips of

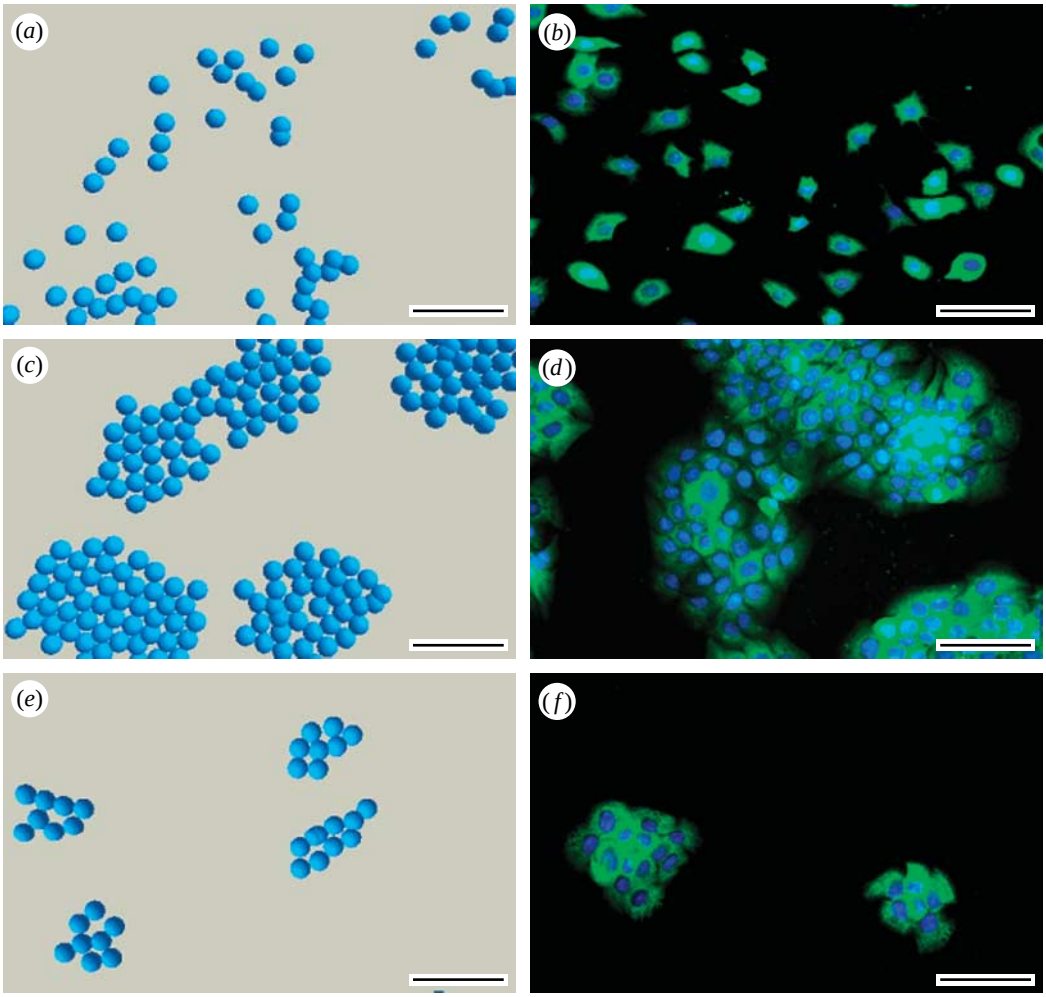

Figure 5. Micrographs of modelled HaCat cells (blue) in (*a*) low (0.09 mM), (*c*) physiological (2 mM) and (*e*) high (4 mM) Ca^{++} environments. Fluorescent micrographs of HaCat cells cultured in (*b*) low (0.09 mM), (*d*) physiological (2 mM) and (*f*) high (4 mM) Ca^{++} environments. The HaCat cells were stained with DAPI (blue) and pancytokeratin antibody (green). Scale bar, 100 μm.

modelling of keratinocyte colony formation in low and physiological Ca^{++}.)

Comparing this simulation of keratinocyte behaviour to the behaviour of the cells *in vitro*, it was found that NHK cells proliferated, migrated actively and distributed evenly throughout the tissue culture surface in a low calcium medium (0.09 mM) as illustrated in figure 2*e*, whereas compact self-limiting colonies were found in the physiological calcium (2 mM) environment as shown in figure 2*f*.

Figure 3*a* shows the total number of modelled TA cells and stem cells when simulated in low and physiological calcium for up to six weeks. Normally, skin cells are only cultured for one to two weeks prior to experimentation or clinical use. With deliberate longer term culture of cells both the *in virtuo* model and the *in vitro* data (figure 3*b*) showed an initial increase in the total viable cell population followed by a much slower decrease in cell number. In the model, the decreasing cell number after the peak value is due to loss of stem cells and TA cells to become committed cells and corneocytes (ultimately corneocytes would be shed from the skin surface hence are not counted in this model). *In vitro* it was found that cells reduced in volume and detached from the culture surface with time—almost certainly following irreversible differentiation. Thus, the initial model predicted the overall pattern of cell number versus time *in vitro*.

However, the timing of the modelled increase did not accurately simulate the *in vitro* increase and decrease seen for cells either in low or physiological calcium. In low calcium levels, viable cell number peaked at around day 7–8 and then subsequently decreased. In physiological calcium level, the greatest number of viable cells was achieved at around day 12. To adjust the model to simulate the biological data, the average cell cycle length can be adjusted as shown in figure 3*c*.

4.2. Identification of key regulation mechanisms

Once we had established an initial model that roughly described the behaviour of the cells *in vitro* both in low and physiological calcium, the model was then used to test the relative importance of some of the literature-derived rules on which the model was based. Firstly, the effect of different cell–cell and cell–substrate adhesiveness on NHK pattern formation was tested in the agent-based model. Weak stem cell–cell bonds resulted in disruption of the stem cell clusters and intermingling of stem, TA and committed cells. A pattern of colony

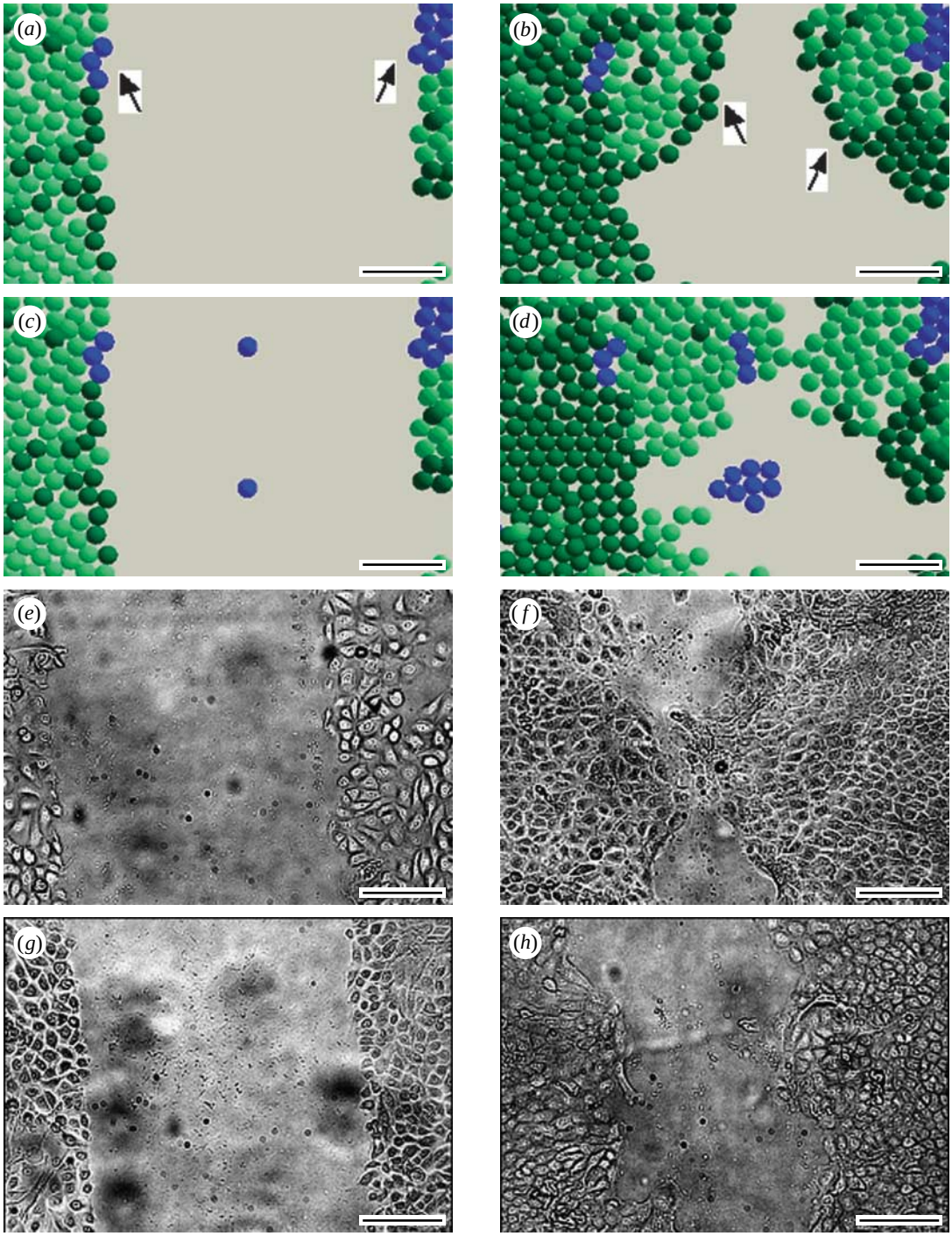

Figure 6. Micrographs of modelled NHK cells in physiological calcium in the bottom layer of (*a*) a scratch wound immediately post created *in virtuo* by removing the cells in the strip, the arrows show the position of stem cell compartments and (*b*) partly healed wound 370 iterations after scratch with slow and quick healing areas predicted by the agent-based model, the arrows show the quick healing areas, (*c*) scratch wound immediately post transplanted with stem cells *in virtuo* and (*d*) partly healed wound 370 iterations after transplanted with stem cells. Phase contrast micrographs of (*e*, *g*) scratch wounds created in confluent NHK cells cultured in physiological Ca^{++} environments, (*f*) quick healing area 24 h after wounding, (*h*) slow healing area 7 days post wounding. Scale bar, 100 μm.

formation was only created when more cohesive bonds were applied between stem cells than between their daughter TA cells. Strong stem cell–substrate interactions were important to keep the stem cell clusters on the substrate. Weak cell–substrate bonds induced the detachment of stem cell niches from the substrate. The crucial roles of cell–cell and cell–substrate bonds of committed cells and corneocytes were also identified by *in virtuo* simulation. These 'failed' simulations are not shown. In contrast, as already stated, figure 3*c* shows the impact of *in virtuo* testing different cell cycle times of stem and TA cells in physiological Ca^{++} media. However, not shown but important to note, varying cell cycle times had no obvious effects on the overall NHK macroscopic morphogenesis produced using this model (which was essentially similar to that seen in figure 2*b*) the influence was solely on the time taken to achieve this pattern.

The next regulatory mechanism that was investigated was the literature suggestion that TA cells only divide 3–5 times *in vivo*. Accordingly, this was applied as a rule to our model. However, this caused early disruption of NHK colony formation in the physiological calcium model and subconfluence of cells in the low calcium model, which differs from what actually occurs in *in vitro* cell culture. An unlimited cell division capacity for TA cells was then applied to the model. This gave a more realistic representation of the behaviour of the cells in the *in vitro* culture and *in virtuo* statistical analysis indicated that the actual average number of divisions that TA cells underwent either in low or physiological Ca^{++} model media was very limited (around 1 in our current model conditions in physiological calcium and less than 1 in low calcium). Further *in virtuo* simulation indicated that varying cell seeding density had no obvious effect on the number of TA cell divisions in physiological calcium. The average TA division was around 1 with a maximum division number of 9. In contrast, increasing cell seeding density in low calcium gradually reduced the average division number of TA cells as shown in figure 3*d*.

One of the predominant issues for TA cell division is space. Early TA cells have plenty of space, and thus can divide a relatively large number of times (leading to the highest maximum division figure calculated from this model of nine divisions). Larger number of TA cells appearing later in the simulation have less and less space, inhibiting possibilities for division (if there is any space to divide at all), thus bringing the average figure for cell division down for the entire simulation. Furthermore, TA cells produced by stem cells on the edge of the stem cell colony are an alternative cell source for the TA cell compartment of the keratinocyte colony; these also reduce the chances of TA cell division. Therefore, for low calcium, the higher the initial seeding density the lower the average number of TA cell divisions. For physiological calcium, TA cell division space is also restricted by the size of the overall colony, since the colony will eventually be 'fenced in' by committed cells. Accordingly, the effect of seeding on TA cell division would not become apparent until seeding levels become high enough for colonies to start competing with one another for space.

4.3. Simulation of HaCat cell dynamic multicellular morphogenesis

HaCaT cells are a spontaneously immortalized human keratinocyte cell line which has been shown to be capable of stratification and expression of epidermal differentiation markers when grafted onto mice (Boukamp *et al.* 1988). However, in *in vitro*, these cells are more proliferative than NHKs in a physiological Ca^{++} environment and have little or no expression of differentiation associated desmosomal cadherin glycoproteins (Denning *et al.* 1998) or other differentiation markers such as defensin (Abiko *et al.* 2003). Nevertheless, exposing these cells to supraphysiological levels of calcium can give rise to expression of these differentiation markers. Research suggests that these cells respond differently to changes in extracellular calcium than NHKs—the intracellular Ca^{++} level (70–100 nM) of HaCats in physiological Ca^{++} environment is much closer to that of NHK cultured in low Ca^{++} media (Sakaguchi *et al.* 2003). However, it can be elevated by increasing extracellular Ca^{++} to supraphysiological levels (Sakaguchi *et al.* 2003). This firmly suggests that HaCat cells are more resistant to the influence of extracellular Ca^{++} probably due to an alteration in a Ca^{++} ion channel or purinoceptor-mediated calcium mobilization (Lee *et al.* 2001).

Accordingly, we explored two hypotheses *in virtuo* to explain the differences in behaviour between HaCats and NHKs. In hypothesis one, we proposed that HaCats are intrinsically blocked from undergoing normal differentiation without taking into account the mechanisms behind it. In hypothesis two, we further proposed that a differing sensitivity to calcium is the key mechanism that explains how HaCat cells differ from NHKs. It was proposed that they have a much higher threshold of extracellular calcium to trigger differentiation.

To explore hypothesis one, the differentiation and stem cell niche mechanisms of the NHK model were simply 'knocked out' when modelling HaCats' behaviour. For hypothesis two, the sensitivity of NHK to calcium was shifted to a higher range to simulate HaCats' responses to different Ca^{++} environments while keeping the differentiation rules unaltered.

Figure 4*a* illustrates that when the possibility of differentiation was omitted (hypothesis one) the increase in viable cell number for HaCats in low and physiological calcium was identical (and very similar to that of NHK in low calcium) with a maximum number of viable cells around modelling time of day 21, numbers decreasing sharply thereafter. Figure 4*b* shows the assessment of total cellular viability for cultures of HaCats grown in low and physiological calcium with a maximum viability around day 9. The growth curves of both *in virtuo* modelling and *in vitro* cell culture share almost the same pattern, which supports the hypothesis that HaCats lack the ability to differentiate whether in low or physiological calcium environments and that this is responsible for the behaviour differences between NHKs and HaCats.

To further explore the mechanism behind hypothesis one, the differentiation mechanism and the sigmoid pattern of NHK's response to extracellular calcium were unaltered, but the sensitivity to calcium was simply shifted to a higher range to simulate HaCats. The extracellular calcium was varied from 0.9 to 6 mM for simulation and *in vitro* cell culture. The results indicated that there is a clear response of the cells to extracellular calcium (as previously reported) predicted by the model (figure 4*c*) and also confirmed by *in vitro* cell culture (figure 4*d*). Most strikingly, this can be seen in the photographs of the simulated cells in 0.09, 2 and 4 mM calcium shown in figure 5*a*,*c* and *e*, comparing these with the actual cells under the same calcium conditions as shown in figure 5*b*,*d* and *f*.

Altering the parameters for the sensitivity of the HaCats to calcium (by a factor of nearly 4) without altering any other rules (the differentiation rule was left intact) in the model gave small tight colony formations.

This simulated the actual colonies obtained at supraphysiological calcium which appeared to be very self-limiting with limited multilayering. Thus, some, albeit abnormal, self-regulation of colony formation was seen at supraphysiological extracellular calcium (please see the website http://www.dcs.shef.ac.uk/~phil/epiresources for movie clips of modelling of HaCat cells in different Ca^{++} environments), indicating that altered calcium sensitivity only partially contributed to the behaviour of HaCat cells. Thus, the data suggest HaCats lack the ability to form NHK type colonies *in vitro* even when supraphysiologically high levels of calcium are present, but further investigation shows there is some remaining response to calcium in these cells as they do achieve increased cell–cell binding at relatively high levels of extracellular calcium.

4.4. Prediction and validation of scratch wound healing in two-dimensional cell culture

We then used the *in virtuo* model for the NHKs to make predictions on how cells would respond to wounding. A simple scratch wound was simulated by removing all of the modelled NHK cells located within a strip (300–400 μm wide) in the centre of confluent modelled cells under different Ca^{++} environments. In a low Ca^{++} media, rapid wound healing was achieved by active cell migration and subsequent cell proliferation (data not shown). Cells moved individually and achieved complete re-epithelialization within 1–2 days of wounding. In contrast, in physiological Ca^{++} media, cells migrated as a coherent sheet.

The model predicted that injuries close to stem or TA cell compartments would heal quickly, whereas very slow wound closure would be achieved in areas containing only committed cells and/or corneocytes as illustrated in figure 6*a*,*b*. The model also predicted that the wound healing process could be accelerated by seeding a small number of stem cells in the denuded area as shown in figure 6*c*,*d*. (Please see the website http://www.dcs.shef.ac.uk/~phil/epiresources for movie clips of modelling of keratinocyte wound healing in low and physiological Ca^{++}.)

In vitro scratch wound-healing experiments were then designed based on these predictions. NHK cells in low Ca^{++} were observed to migrate freely into the denuded area to close the wound within 24 h in the low Ca^{++} media (results not shown). In physiological Ca^{++}, however, the wound edge was observed to migrate as a contiguous sheet with significantly different rates: in some areas rapid wound healing was observed within 24 h (figure 6*e*,*f*), while in other areas there was no sign of complete healing even after 7 days of culture (figure 6*g*,*h*). The rapidly healing areas were identified as germinative compartments with high rates of BrdU incorporation (indicative of proliferation) (figure 7*a*,*b*) and low levels of involucrin expression (indicative of differentiation; figure 7*c*). In contrast, the slow or non-healing areas were identified as committed cell compartments with low rates of BrdU incorporation (figure 7*d*,*e*) and high levels of involucrin expression as illustrated in figure 7*f*.

5. DISCUSSION

The regulation of epidermal homeostasis involves a complex interplay between different generic and genetic mechanisms, making it difficult to investigate except by focusing on separate discrete aspects of the biology. In agent-based computational model, individual cells are represented by autonomous software agents, which execute a set of rules according to cell internal states and immediate environments. This has the advantage of creating a global view of the macroscopic morphogenesis of NHK cells *in virtuo*, allowing the testing of hypotheses and designing of new and informative experiments.

Previously, we developed a cell-based computational model for urothelial cells in monolayer culture (Walker *et al.* 2004*a*,*b*). However, extension of this model to NHK and HaCat cell demonstrated some of its limitations (Walker *et al.* 2006) suggesting it did not include sufficient biological rules. Another agent-based model has recently been developed to simulate and predict epidermal morphology, tissue kinetics and the two-dimensional flow of calcium ions (Grabe & Neuber 2005). In this model, the keratinocyte differentiation mechanism was assumed to be solely based on the calcium levels.

Our aim in the current study was to develop and validate a model of epidermal cell social behaviour, which would be accessible for use by cell biologists interested in questions of epidermal organization and homeostasis. In establishing this agent-based model, we found we had to change initial assumptions about keratinocyte TA cell division and the length of cell cycle in different calcium media. We then tested two different hypotheses about how the growth of the HaCat keratinocyte cell line differed from NHKs. Two hypotheses were proposed: the first was that HaCats are intrinsically incapable of normal colony formation irrespective of the calcium concentration and the second was that these cells had an altered (abnormally so) calcium sensitivity. Both hypotheses were supported—the first to a greater extent than the second. This suggests that cells fail to differentiate for reasons which include but are not fully explained by an altered sensitivity to calcium. In this research, we also predicated and validated a position-dependent scratch wound healing pattern of keratinocytes in monolayer culture. The development of the model is described in this study and access to this software model can be obtained via our website as mentioned earlier.

In brief, we suggest that the initial validation of the model seems promising and has quickly led to the generation of hypotheses for exploration. The hypotheses we describe are only a few of the questions that can now be tackled using this model.

Firstly, to summarize the main outcomes of the model, we found that cell–cell and cell–substrate mediated contacts were crucially important for the colony-forming pattern of NHK cells in physiological calcium. These results, while important, are as expected. Other outcomes were less predictable—the basic model rules simulated the initial increase and then decrease in total viable cell number seen when cells were grown for up to six weeks. However, it was necessary to alter the cell cycle length of the cells to

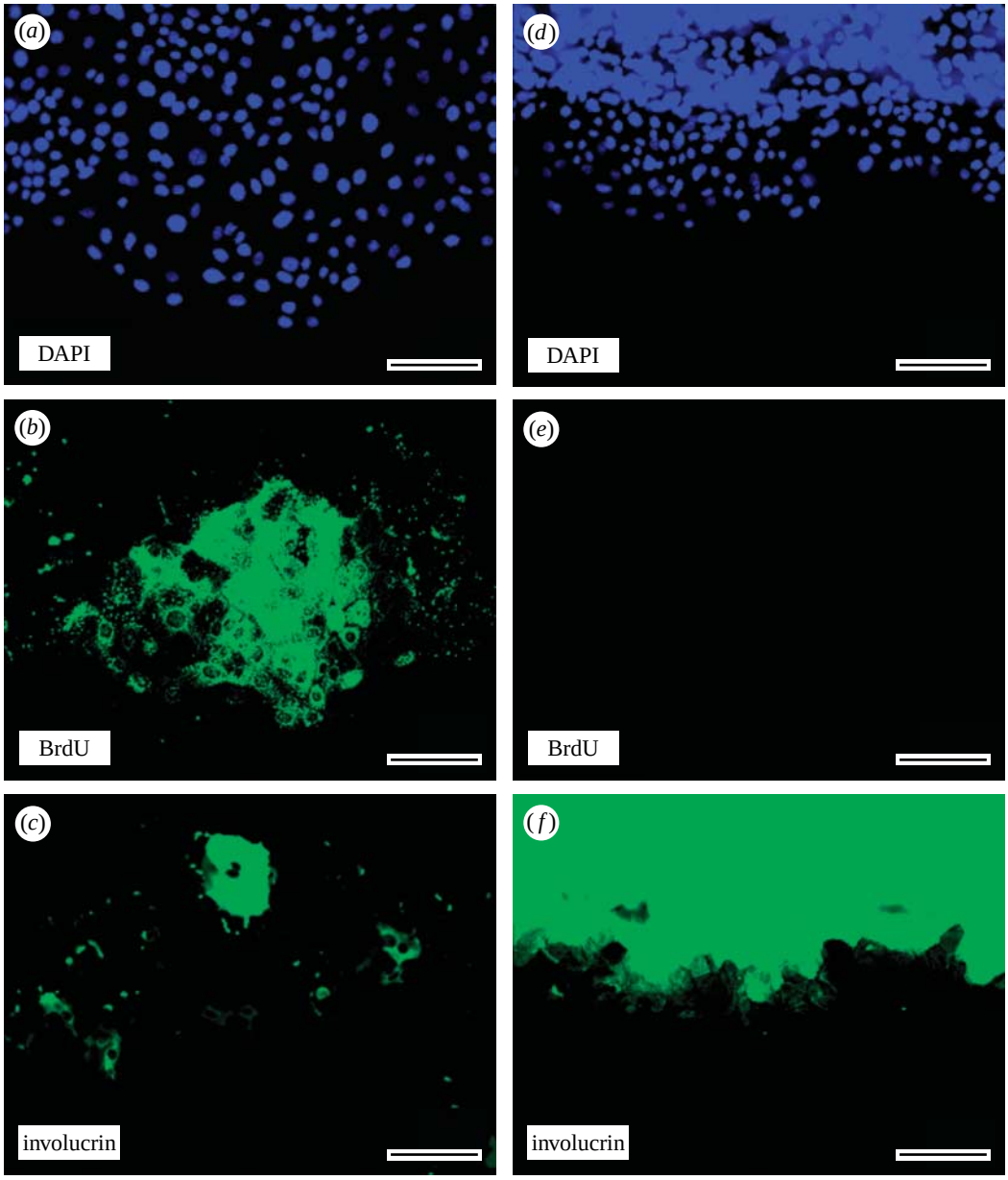

Figure 7. Fluorescent micrographs of NHK in physiological calcium in a scratch wound model with (*a*) cell nuclei stained with DAPI (blue), (*b*) cells incorporating BrdU and (*c*) cells which expressed involucrin in quick healing areas. In contrast, (*d*) shows cell nuclei stained with DAPI and (*e*) cells failing to incorporate BrdU (*f*) cells expressing involucrin in a slow healing area within the same culture. Scale bar, 100 μm.

reflect the more rapid or slow increase in cell number. The next finding was that the literature suggests that TA cells can divide only 3–5 times (Dover & Wright 1991; Jensen *et al.* 1999; Lowell *et al.* 2000; Okuyama *et al.* 2004; Kolly *et al.* 2005). Data from the model however suggested that the limited division ability of TA cells was not an intrinsic cell property of the cells but rather a statistical phenomenon. In the model, TA cells were allowed to divide without any limitation. However, it became apparent that whereas some cells (those TA cells arising from stem cells early in colony formation) might divide up to a maximum number of nine times, other TA cells did not divide at all (largely due to space limitations in low calcium or to parameters limiting the size of the colonies in physiological calcium). Thus, the model showed that the average TA cell division time was around 1 in physiological calcium and less than 1 in low calcium under current simulation conditions. These data strongly suggest that TA cells divide according to 'need' or opportunity, rather than it being an inherent property of the cell.

Another interesting finding related to the length of the cell cycle. The lack of methods to identify and measure cell cycle times of TA cells and stem cells is frustrating for biologists but here, interestingly, investigation *in virtuo* showed that varying the cell cycle times of stem or TA cells had no obvious effects on macroscopic morphogenesis. Essentially, different cycle times had no overall effect on the final structure of the colonies, they simply affected the length of time required to achieve this structure.

The model was then extended to see if we could simulate the behaviour of the HaCat keratinocyte cell line. HaCat cells are a useful keratinocyte cell line in

that they behave as though they are undifferentiated TA cells even in physiological Ca^{++} environments. Thus, they are easy to expand and culture without going into terminal differentiation. However, the literature suggests that these cells have at least some capacity for terminal differentiation when they are implanted *in vivo* on nude mice (Boukamp *et al.* 1988). Also previous work has suggested that one of their major differences to NHK cells is their sensitivity to extracellular calcium (Sakaguchi *et al.* 2003). As discussed earlier, calcium is clearly key to helping initiate differentiation (although not the only factor) but crucial to allow differentiation to complete in NHKs. Thus, if for whatever reason the intracellular calcium of HaCats does not rise to the permissive levels required for differentiation, then this could explain their behaviour to a large extent.

Two alternative hypotheses to explain HaCat cell *in vitro* behaviour were explored: an intrinsic abnormality in their ability to differentiate and an abnormality in their calcium regulation. The first was simulated by knocking out mechanisms for differentiation and stem cell niche autoregulation. This then produced an *in virtuo* model which simulated the behaviour of the HaCats in physiological calcium. The growth curves of both *in virtuo* modelling and *in vitro* cell culture share almost the same pattern, which supports the hypothesis. The second hypothesis that the mechanisms for differentiation and stem cell niche autoregulation would start to function if HaCat cells were exposed to a superphysiological level of extracellular calcium was then explored. The *in vitro* experimentation revealed that if cultured in sufficiently high calcium media HaCat cell proliferation decreased and cells began to form compact colonies. However, these were still clearly and visibly different to NHK colonies (no stratification of cells in these very tight HaCaT colonies) but nevertheless this hypothesis was supported to a certain extent. We suggest that the modelling supports cells having a clear abnormality in their calcium responsiveness (as already supported by the current literature) but also some additional defect in their ability to differentiate beyond this.

The *in virtuo* model for colony formation in NHKs was then tested further by making a wound (equivalent to a scratch wound) in a monolayer culture of NHKs. The modelling revealed that active cell migration and subsequent cell proliferation contributed to the rapid wound closure in a low Ca^{++} media, whereas in physiological calcium media wound healing was very dependant on the position of the wound with respect to the nearest stem cells or TA cells. At this stage, the model was used to design *in vitro* scratch wound experiments to examine to what extent this hypothesis would hold true. We were able to show, within the same scratch wound, areas of rapid wound healing and areas of slow wound healing. Rapid healing turned out to be attributable to actively proliferating keratinocytes (germinative compartments) and areas of very slow wound healing were associated with cells in the same culture showing low levels of proliferation and relatively high levels of differentiation. We suggest this confirms the prediction from the *in virtuo* modelling.

In tissue development, cells actively change their behaviour and properties, as a consequence of internal decisions due to 'rules' that are encoded in the genetic information of each cell. These have been selected throughout evolution and are influenced by the immediate environments. Hence, a model that permits prediction of individual cells or multicellular behaviour should combine a description of a cell with a description of the rules that dictate the change of its behaviour or parameters (Baker *et al.* 1998; Hogeweg 2000*a*,*b*; Drasdo & Hohme 2005; Galle *et al.* 2005; Ponciano *et al.* 2005). This goes beyond the work described in this study in which we have a model that describes the spatial growth pattern of keratinocytes determined by the relationship between individual cells evolving with time. At this stage of development, the model does not incorporate detailed intracellular information, nor does it deal with the cells' responses to a wide range of external agents (but, in principle, any rule in the model could be replaced by a model of the mechanism underlying the rule). The model does allow us to begin to see organization of cells in three dimensions (in physiological calcium) and most importantly allows one to test different hypotheses of how cells will respond to basic features of cell manipulation *in vitro*.

Now that this basic model has been established, there are significant further challenges to be taken on in terms of looking at the interaction of the keratinocytes with stromal fibroblasts and then progressively adding in more details wherever the model indicates particular parameters are particularly important (such as in cell–cell adhesion for example). However, the model at this stage can be used to explore many of the questions which keratinocyte biologists currently answer at an empirical level. Thus, it should now be possible to predict why certain seeding densities of keratinocytes will get a better expansion of cells than others, why passaging cells at a certain density and after a certain length of culture yield more proliferative cells than under other conditions and how to manipulate the extracellular calcium environment to get best value from biopsies of patient cells for clinical expansion.

In summary, in this study, we have described a novel computational model of keratinocyte colony formation. Since the model treats cells as individual entities it can be tightly coupled to experimental work, enabling hypotheses to be readily generated and tested. Our study shows that this synergy between computational and experimental models has the potential to become a powerful tool for understanding how cells organize into tissue

We gratefully acknowledge financial support from EPSRC (UK) for this research.

REFERENCES

Abiko, Y., Nishimura, M., Kusano, K., Yamazaki, M., Arakawa, T., Takuma, T. & Kaku, T. 2003 Upregulated expression of human β defensin-1 and -3 mRNA during

differentiation of keratinocyte immortalized cell lines, HaCaT and PHK16-0b. *J. Dermatol. Sci.* **31**, 225–228. (doi:10.1016/S0923-1811(03)00007-0)

Adams, J. C. & Watt, F. M. 1990 Changes in keratinocyte adhe sion during terminal differentiation: reduction in fibronectin binding precedes alpha 5 beta 1 integrin loss from the cell surface. *Cell* **63**, 425–435. (doi:10.1016/0092-8674(90)90175-E)

Aplin, A. E., Howe, A. K. & Juliano, R. L. 1999 Cell adhesion molecules, signal transduction and cell growth. *Curr. Opin. Cell Biol.* **11**, 737–744. (doi:10.1016/S0955-0674(99)00045-9)

Ashkenas, J., Muschler, J. & Bissell, M. J. 1996 The extracellular matrix in epithelial biology: shared molecules and common themes in distant phyla. *Dev. Biol.* **180**, 433–444. (doi:10.1006/dbio.1996.0317)

Asplund, A., Guo, Z., Hu, X., Wassberg, C. & Ponten, F. 2001 Mosaic pattern of maternal and paternal keratinocyte clones in normal human epidermis revealed by analysis of X-chromosome inactivation. *J. Invest. Dermatol.* **117**, 128–131. (doi:10.1046/j.0022-202x.2001.01385.x)

Assoian, R. K. 1997 Anchorage-dependent cell cycle progression. *J. Cell Biol.* **136**, 1–4. (doi:10.1083/jcb.136.1.1)

Baker, C. T. H., Bocharov, G. A., Paul, C. A. H. & Rihan, F. A. 1998 Modelling and analysis of time-lags in some basic patterns of cell proliferation. *J. Math. Biol.* **37**, 341–371. (doi:10.1007/s002850050133)

Balanescu, T., Cowling, A. J., Georgescu, H., Gheorghe, M., Holcombe, M. & Vertan, C. 1999 Communicating stream X-machines systems are no more than X-machines. *J. Univ. Comput. Sci.* **5**, 494–507.

Baumgarter, W., Hinterdorfer, P., Ness, W., Raab, A., Vestweber, D., Schindler, H. & Drenckhahn, D. 2000 Cadherin interaction probed by atomic force microscopy. *Proc. Natl Acad. Sci. USA* **97**, 4005–4010. (doi:10.1073/pnas.070052697)

Bhadriraju, K. & Hansen, L. K. 2004 Extracellular matrix-dependent myosin dynamics during G1-S phase cell cycle progression in hepatocytes. *Exp. Cell Res.* **300**, 259–271. (doi:10.1016/j.yexcr.2004.06.033)

Bhatia, S. N., Balis, U. J., Yarmush, M. L. & Toner, M. 1999 Effect of cell–cell interactions in preservation of cellular phenotype: cocultivation of hepatocytes and nonparenchymal cells. *FASEB J.* **13**, 1883–1900.

Boukamp, P., Petrussevska, R. T., Breitkreutz, D., Hornung, J., Markham, A. & Fusenig, N. E. 1988 Normal keratinization in a spontaneously immortalized aneuploid human keratinocyte cell line. *J. Cell Biol.* **106**, 761–771. (doi:10.1083/jcb.106.3.761)

Coakley, S., Smallwood, R. & Holcombe, M. 2006 Using X-machines as a formal basis for describing agents in agent-based modeling. In *Proc. Agent-Directed Simulation* (*ADS*'06) *Conference,* 2–6 *April.*

Cox, E. A., Sastry, S. K. & Huttenlocher, A. 2001 Integrin-mediated adhesion regulates cell polarity and membrane protrusion through Rho family of GTPases. *Mol. Biol. Cell* **12**, 265–277.

Croix, B. S., Sheehan, C., Rak, J. W., Florenes, V. A., Slingerland, J. M. & Kerbel, R. S. 1998 E-Cadherindependent growth suppression is mediated by the cyclin-dependent kinase inhibitor p27 KIPI. *J. Cell Biol.* **142**, 557–571. (doi:10.1083/jcb.142.2.557)

Dalrymple, S., Antony, L., Xu, Y., Uzgare, A. R., Arnold, J. T., Savaugeot, J., Sokoll, L. J., Marzo, A. M. D. & Isaacs, J. T. 2005 Role of Notch-1 and E-Cadherin in the differential response to calcium in culturing normal versus malignant prostate cells. *Cancer Res.* **65**, 9269–9279. (doi:10.1158/0008-5472.CAN-04-3989)

Denning, M. F., Guy, S. G., Ellerbroek, S. M., Norvell, S. M., Kowalczyk, A. P. & Green, K. J. 1998 The expression of desmoglein isoforms in cultured human keratinocytes is regulated by calcium, serum, and protein kinase C. *Exp. Cell Res.* **239**, 50–59. (doi:10.1006/excr.1997.3890)

DiMilla, P. A., Barbee, K. & Lauffenburger, D. A. 1991 Mathematical model for the effects of adhesion and mechanics on cell migration speed. *Biophys. J.* **60**, 15–37.

Dover, R. & Potten, C. S. 1983 Cell cycle kinetics of cultured human epidermal keratinocytes. *J. Invest. Dermatol.* **80**, 423–429. (doi:10.1111/1523-1747.ep12555494)

Dover, R. & Wright, N. A. 1991 The cell proliferation kinetics of the epidermis. In *Physiology, biochemistry and molecular biology of the skin* (ed. L. A. Goldsmith), pp. 239–265. Oxford, UK: Oxford University Press.

Drasdo, D. & Hohme, S. 2005 A single-cell-based model of tumor growth *in vitro*: monolayers and spheroids. *Phys. Biol.* **2**, 133–147. (doi:10.1088/1478-3975/2/3/001)

Eglen, S. J. & Willshaw, D. J. 2002 Influence of cell fate mechanisms upon retinal mosaic formation: a modelling study. *Development* **129**, 5399–5408. (doi:10.1242/dev.00118)

Fleischmajer, R. *et al.* 2000 Differential expression of laminin α chains during proliferative and differentiation stages in a model for skin morphogenesis. *Matrix Biol.* **19**, 637–647. (doi:10.1016/S0945-053X(00)00092-5)

Galle, J., Loeffler, M. & Drasdo, D. 2005 Modeling the effect of deregulated proliferation and apoptosis on the growth dynamics of epithelial cell populations *in vitro*. *Biophys. J.* **88**, 62–75. (doi:10.1529/biophysj.104.041459)

Gizelda, T. B., Wieser, R., Bunge, R. P., Margitich, I. S., Katz, J., Olson, L. & Wood, P. M. 2000 Density dependent regulation of human Schwann cell proliferation. *Glia* **30**, 165–177. (doi:10.1002/(SICI)1098-1136(200004)30:2<165::AID-GLIA6>3.0.CO;2-L)

Goulet, F., Poitras, A., Rouabhia, M., Cusson, D., Germain, L. & Auger, F. A. 1996 Stimulation of human keratinocyte proliferation through growth factor exchanges with dermal fibroblasts *in vitro*. *Burns* **22**, 107–112. (doi:10.1016/0305-4179(95)00098-4)

Grabe, N. & Neuber, K. 2005 A multicellular systems biology model predicts epidermal morphology, kinetics and Ca 2+ flow. *Bioinformatics* **21**, 3541–3547. (doi:10.1093/bioinformatics/bti585)

Grossmann, J., Walther, K., Artinger, M., Kiessling, S. & Scholmerich, J. 2001 Apoptotic signaling during initiation of detachment-induced apoptosis ("Anoikis") of primary human intestinal epithelial cells. *Cell Growth Differ.* **12**, 147–155.

Hogeweg, P. 2000*a* Evolving mechanisms of morphogenesis: on the interplay, between differential adhesion and cell differentiation. *J. Theor. Biol.* **203**, 317–333. (doi:10.1006/jtbi.2000.1087)

Hogeweg, P. 2000*b* Shapes in the shadow: evolutionary dynamics of morphogenesis. *Artif. Life* **6**, 85–101. (doi:10.1162/106454600568339)

Holbrook, K. A. 1994 Ultrastructure of the epidermis. In *The keratinocyte handbook* (eds I. M. Leigh, B. Lane & F. M. Watt), pp. 3–39. London, UK: Cambridge University Press.

Ingber, D. E. 2003*a* Tensegrity I. Cell structure and hierarchical systems biology. *J. Cell Sci.* **116**, 1157–1173. (doi:10.1242/jcs.00359)

Ingber, D. E. 2003*b* Tensegrity II. How structural networks influence cellular information processing networks. *J. Cell Sci.* **116**, 1397–1408. (doi:10.1242/jcs.00360)

Jensen, U. B., Lowell, S. & Watt, F. M. 1999 The spatial relationship between stem cells and their progeny in the

basal layer of human epidermis: a new view based on whole-mount labelling and lineage analysis. *Development* **126**, 2409–2418.

Kefalas, P., Holcombe, M., Eleftherakis, G. & Gheorghe, M. 2003 A formal method for the development of agent-based systems. In *Intelligent agent software engineering* (ed. V. Plekhavona), pp. 68–98. Hershey, PA: Idea Group Publishing.

King, K. L. & Cidlowski, J. A. 1995 Cell cycle and apoptosis: common pathways to life and death. *J. Cell. Biochem.* **58**, 175–180. (doi:10.1002/jcb.240580206)

Kolettas, E., Skoufos, I., Kontargiris, E., Markopoulou, S., Tzavaras, T. & Gonos, E. S. 2006 Bcl-2 but not clusterin/apolipoprotein J protected human diploid fibroblasts and immortalized keratinocytes from ceramide-induced apoptosis: role of p53 in the ceramide response. *Arch. Biochem. Biophys.* **445**, 184–195. (doi:10.1016/j.abb.2005.10.006)

Kolly, C., Suter, M. M. & Muller, E. J. 2005 Proliferation, cell cycle exit, and onset of terminal differentiation in cultured keratinocytes: pre-programmed pathways in control of C-Myc and Notch 1 prevail over extracellular calcium signals. *J. Invest. Dermatol.* **124**, 1014–1025. (doi:10.1111/j.0022-202X.2005.23655.x)

Korang, K., Christiano, A. M., Uitto, J. & Mauviel, A. 1995 Differerential cytokine modulation of the genes LAMA3, LAMB3, and LAMC2, encoding the constitutive polypeptides, α3, β3, and γ2, of human laminin 5 in epidermal keratinocytes. *FEBS Lett.* **368**, 556–558. (doi:10.1016/0014-5793(95)00740-Z)

Laporte, M. & Heenen, M. 1994 The heterogeneity of the germinative compartment in human epidermis and its implications in pathogenesis. *Dermatology* **189**, 340.

Latkowski, J. A. M., Freedberg, I. M. & Blumenberg, M. 1995 Keratinocyte growth factor and keratin gene regulation. *J. Dermatol. Sci.* **9**, 36–44. (doi:10.1016/0923-1811(94)00350-N)

Lee, W. K., Choi, S. W., Lee, H. R., Lee, E. J., Lee, K. H. & Kim, H. O. 2001 Purinoceptor-mediated calcium mobilization and proliferation in HaCaT keratinocytes. *J. Dermatol. Sci.* **25**, 97–105. (doi:10.1016/S0923-1811(00)00117-1)

Lowell, S., Jones, P., Roux, I. L., Dune, J. & Watt, F. M. 2000 Stimulation of human epidermal differentiation by Delta-Notch signalling at the boundaries of stem-cell clusters. *Curr. Biol.* **10**, 491–500. (doi:10.1016/S0960-9822(00)00451-6)

MacArthur, B. D., Please, C. P., Taylor, M. & Oreffo, R. O. C. 2004 Mathematical modelling of skeletal repair. *Biochem. Biophys. Res. Commun.* **313**, 825–833. (doi:10.1016/j.bbrc.2003.11.171)

Meineke, F. A., Potten, C. S. & Loeffler, M. 2001 Cell migration and organization in the intestinal crypt using a lattice-free model. *Cell Prolif.* **34**, 253–266. (doi:10.1046/j.0960-7722.2001.00216.x)

Morel, D., Marcelpoil, R. & Brugal, G. 2001 A proliferation control network model: the simulation of two-dimensional epithelial homeostasis. *Acta Biotheoretica* **49**, 219–234. (doi:10.1023/A:1014201805222)

Nelson, C. M. & Chen, C. S. 2002 Cell–cell signaling by direct contact increases cell proliferation via a PI3K-dependent signal. *FEBS Lett.* **514**, 238–242. (doi:10.1016/S0014-5793(02)02370-0)

Nelson, C. M., Jean, R. P., Tan, J. L., Liu, W. F., Sniadecki, N. J., Spector, A. A. & Chen, C. S. 2005 Emergent patterns of growth controlled by multicellular form and mechanics. *Proc. Natl Acad. Sci. USA* **102**, 11 594–11 599. (doi:10.1073/pnas.0502575102)

Nishimura, E. K., Yoshida, H., Kunisada, T. & Nishikawa, S. I. 1999 Regulation of E- and P-cadherin expression correlated with melanocyte migration and diversification. *Dev. Biol.* **215**, 155–166. (doi:10.1006/dbio.1999.9478)

Okuyama, R., LeFort, K. & Dotto, G. P. 2004 A dynamic model of keratinocyte stem cell renewal and differentiation: role of the p21WAF1/Cip1 and Notch 1 signaling pathways. *J. Invest. Dermatol. Symp. Proc.* **9**, 248–252. (doi:10.1111/j.1087-0024.2004.09308.x)

Olsson, L. 2003 Cell migration, pattern formation and cell fate during head development in lungfishes and amphibians. *Theory Biosci.* **122**, 252–265. (doi:10.1078/1431-7613-00086)

Orford, K., Orford, C. C. & Byers, S. W. 1999 Exogenous expression of beta-catenin regulates contact inhibition, anchorage-independent growth, anoikis and radiation-induced cell cycle arrest. *J. Cell Biol.* **146**, 855–867. (doi:10.1083/jcb.146.4.855)

Ponciano, J. M., Vandecasteele, F. P. J., Hess, T. F., Forney, L. J., Crawford, R. L. & Joyce, P. 2005 Use of stochastic models to assess the effect of environmental factors on microbial growth. *Appl. Environ. Microbiol.* **71**, 2355–2364. (doi:10.1128/AEM.71.5.2355-2364.2005)

Potten, C. S. & Booth, C. 2002 Keratinocyte stem cells: a commentary. *J. Invest. Dermatol.* **119**, 888–899. (doi:10.1046/j.1523-1747.2002.00020.x)

Rashbass, J. 1996 Modelling tissues on the computer. *Trends Cell Biol.* **6**, 280–281. (doi:10.1016/0962-8924(96)60028-2)

Sakaguchi, M., Miyazaki, M., Takaishi, M., Sakaguchi, Y., Makino, E., Kataoka, N., Yamada, H., Namba, M. & Huh, N. 2003 S100C/A11 is a key mediator of Ca2+ induced growth inhibition of human epidermal keratinocytes. *J. Cell Biol.* **163**, 825–835. (doi:10.1083/jcb.200304017)

Santini, M. T., Rainaldi, G. & Indovina, P. L. 2000 Apoptosis, cell adhesion and extracellular matrix in the three-dimensional growth of multicellular tumor spheroids. *Crit. Rev. Oncol. Hematol.* **36**, 75–87.

Savill, N. J. 2003 Mathematical models of hierarchically structured cell populations under equilibrium with application to the epidermis. *Cell Prolif.* **36**, 1–26. (doi:10.1046/j.1365-2184.2003.00257.x)

Savill, N. J. & Sherratt, J. A. 2003 Control of epidermal stem cell clusters by Notch-mediated lateral induction. *Dev. Biol.* **258**, 141–153. (doi:10.1016/S0012-1606(03)00107-6)

Scheffrahn, I., Singer, B. B., Sigmundsson, K., Lucka, L. & Obrink, B. 2005 Control of density-dependent, cell state-specific signal transduction by the cell adhesion molecule CEACAM1, and its influence on cell cycle regulation. *Exp. Cell Res.* **307**, 427–435. (doi:10.1016/j.yexcr.2005.03.030)

Shraiman, B. I. 2005 Mechanical feedback as a possible regulator of tissue growth. *Proc. Natl Acad. Sci. USA* **102**, 3318–3323. (doi:10.1073/pnas.0404782102)

Smola, H., Stark, H.-J., Thiekötter, G., Mirancea, N., Krieg, T. & Fusenig, N. E. 1998 Dynamics of basement membrane formation by keratinocyte–fibroblast interactions in organotypic skin culture. *Exp. Cell Res.* **239**, 399–410. (doi:10.1006/excr.1997.3910)

Sun, T., Mai, S., Haycock, J., Ryan, A. & MacNeil, S. 2005 Self-organisation of skin cells in 3D-electrospun polystyrene scaffolds. *Tissue Eng.* **11**, 1023–1033. (doi:10.1089/ten.2005.11.1023)

Thompson, C. B. 1995 Apoptosis in the pathogenesis and treatment of disease. *Science* **267**, 1456–1462. (doi:10.1126/science.7878464)

Vespa, A., DSouza, S. J. A. & Dagnino, L. 2005 A novel role for integrin-linked kinase in epithelial sheet morphogenesis. *Mol. Biol. Cell* **16**, 4084–4095. (doi:10.1091/mbc.E05-02-0087)

Walker, D. C., Southgate, J., Hill, G., Holcombe, M., Hose, D. R., Wood, S. M., MacNeil, S. & Smallwood, R. H. 2004*a* The epitheliome: agent-based modelling of the social behaviour of cells. *BioSystems* **76**, 89–100. (doi:10.1016/j.biosystems.2004.05.025)

Walker, D. C., Hill, G., Wood, S. M., Smallwood, R. H. & Southgate, J. 2004*b* Agent-based computational modeling of wounded epithelial cell monolayers. *IEEE Trans. Nanobiosci.* **3**, 153–163. (doi:10.1109/TNB.2004.833680)

Walker, J. L., Fournier, A. K. & Assoian, R. K. 2005 Regulation of growth factor signaling and cell cycle progression by cell adhesion and adhesion-dependent changes in cellular tension. *Cytokine Growth Factor Rev.* **16**, 395–405. (doi:10.1016/j.cytogfr.2005.03.003)

Walker, D., Sun, T., MacNeil, S. & Smallwood, R. 2006 Modelling the effect of exogenous calcium on keratinocyte and HaCat cell proliferation and differentiation using an agent-based computational paradigm. *Tissue Eng.* **12**, 2301–2309. (doi:10.1089/ten.2006.12.2301)

Wang, X., Bregegere, F., Soroka, Y., Kayat, A., Redziniak, G. & Milner, Y. 2004 Enhancement of Fas-mediated apoptosis in aging human keratinocytes. *Mech. Aging Dev.* **125**, 237–249. (doi:10.1016/j.mad.2003.12.007)

Webb, A., Li, A. & Kaur, P. 2004 Location and phenotype of human adult keratinocyte stem cells of the skin. *Differentiation* **72**, 387–395. (doi:10.1111/j.1432-0436.2004.07208005.x)

Zaman, M. H., Kamm, R. D., Matsudaira, P. & Lauffenburger, D. A. 2005 Computational model for cell migration in three-dimensional matrices. *Biophys. J.* **89**, 1389–1397. (doi:10.1529/biophysj.105.060723)

Zhu, A. J., Haase, I. & Watt, F. M. 1999 Signaling via β1 integrins and mitogen activated protein kinase determines human epidermal stem cell fate *in vitro*. *Proc. Natl Acad. Sci. USA* **96**, 6728–6733. (doi:10.1073/pnas.96.12.6728)